



Full length article

Saharan, Aral-Caspian and Middle East dust travels to Finland (1980–2022)



György Varga ^{a,b,c,f,*}, Outi Meinander ^d, Ágnes Rostási ^{e,f}, Pavla Dagsson-Waldhauserova ^{g,h}, Adrienn Csávics ^{a,b,c}, Fruzsina Gresina ^{a,b,c,i}

^a HUN-REN Research Centre for Astronomy and Earth Sciences, Budapest, Hungary

^b ELTE Eötvös Loránd University, Institute of Geography and Earth Sciences, Department of Meteorology, Budapest, Hungary

^c CSFK, MTA Centre of Excellence, Budapest, Hungary

^d Atmospheric Composition Research, Finnish Meteorological Institute, Helsinki, Finland

^e MTA-PE Air Chemistry Research Group, Veszprém, Hungary

^f Research Institute of Biomolecular and Chemical Engineering, University of Pannonia, Veszprém, Hungary

^g Faculty of Environmental and Forest Sciences, Agricultural University of Iceland, Reykjavík, Iceland

^h Faculty of Environmental Sciences, Department of Water Resources and Environmental Modeling, Czech University of Life Sciences Prague, Prague, Czech Republic

ⁱ ELTE Eötvös Loránd University, Institute of Geography and Earth Sciences, Department of Environmental and Landscape Geography, Budapest, Hungary

ARTICLE INFO

Handling Editor: Xavier Querol

Keywords:

Finland
Atmospheric dust
Sahara
Meridional transport

ABSTRACT

Studies on atmospheric dust and long-range transport of mineral dust have been a focus of atmospheric science in recent years. With its wide range of direct and indirect effects, mineral dust is one of the most uncertain elements in the mechanisms of climate change, and a deeper understanding of its role is essential for understanding future processes.

The aim of our research was to provide the first systematic data on the so far episodically documented northward transport mineral dust from arid-semiarid areas. So, in this paper, we present dust storm events from lower latitudes reaching the Finnish atmosphere, based on the MERRA-2 model Dust Column Mass Density data and after a multistep verification procedure using independent data source. In total, 86 long-range dust storm events were identified between 1980 and 2022, when air masses loaded with dust reached Finland. Based on backward-trajectories different sources were identified: 59 were Saharan, 22 were Aral-Caspian, and five were associated with Middle Eastern source areas. Considerable variation in inter-annual frequencies was observed among the source areas, which may be due to changes in circulation conditions and the effects of human activity (agriculture and land use changes in Aral Sea region).

There is a clear maximum of dust events in spring (60%), followed by summer and autumn (where 10 of the 11 autumn episodes were from the Sahara). However, the number and proportion of scarce winter events have more than doubled since 2010 compared to the preceding 30 years, but no autumn events were registered during this period. This clear temporal variation coincides with changes in dust transport observed in other regions of Europe, driven by greater atmospheric meridionality associated with climate change and driven by reduced temperature difference between low and high latitudes due to enhanced temperature increases at Arctic regions.

1. Introduction

With the growing frequency of extreme weather events due to today's climate change, research on the unusual mechanisms of the atmosphere has become increasingly important (Easterling et al., 2000; IPCC, 2022; Shepherd, 2014). According to reports by the Intergovernmental Panel on Climate Change, the radiative and other climatic effects of aerosol and especially mineral dust as atmospheric constituents add further uncertainty to changing atmospheric processes and their

predictions. Today, dust emissions from arid and semi-arid areas exceed 3–4 billion tonnes per year (Ginoux et al., 2001; Huneeus et al., 2011). Most of this dust is associated with Saharan sources, but there are also intense emissions in Arabia, Central Asia, the southwestern United States and Australia (Prospero, 2002). In terms of their physical geography, dust sources are typically associated with former or ephemeral lacustrine and fluvial environments (Ginoux et al., 2012).

Aerosol particles, including mineral dust, are active components of our Earth's climate and other environmental systems. As a direct effect,

* Corresponding author at: HUN-REN Research Centre for Astronomy and Earth Sciences, Budapest, Hungary.

E-mail address: varga.gyorgy@csfk.org (G. Varga).

they modify the energy balance through the absorption and scattering of incoming short-wave and terrestrial long-wave radiation, coupled with their significant role in cloud formation and albedo modification processes, which are listed among the indirect radiative effects. Terrestrial and aquatic biogeochemical cycles and productivity, and hence the climate, are also modified by essential nutrient deposition during dust events. Increased concentrations of atmospheric particulate matter can also lead to health problems and non-compliance with environmental directives (e.g., exceeding the European Union standards for PM2.5 and PM10); this is of course mainly the case in areas relatively close to source areas, (e.g., in southern Europe, in Spain, Italy, Greece. Beside these effects, atmospheric and deposited dust could influence the cloud properties, precipitation acidity, lake salinity, soil formation, traffic, and photovoltaic energy production (Monteiro et al., 2022).

Recently there has been an increased interest in long range transport of dust to high latitude (Bullard et al., 2016; Francis et al., 2018, 2019; Di Biagio et al., 2022; Meinander et al., 2022a). This priority is driven by the above-average warming and vulnerability of Arctic regions and albedo changes in snow-ice covered areas, which are identified as potential tipping points in climate projections. The study of atmospheric mineral dust transport episodes from the south to the Arctic, through direct and indirect modification of irradiance and via the warm advection, can provide valuable contributions to all these topics.

Although there are many highly active dust source regions at high latitudes, their activity their emission intensity and frequency are less intense than low latitudes, especially in the Sahara. Studies on the transport of Saharan dust northwards have covered almost every region of Europe (Ginoux et al., 2004; Stuut et al., 2009), from the Mediterranean through Central Europe to Iceland (Varga et al., 2021) and even Greenland (Francis et al., 2019). Saharan dust storm events, i.e., when Saharan dust appears in the atmosphere of a given geographical area, are sporadic but also known from the Nordic region. There is relatively little data on long-range dust storm events in northern Europe. Lundqvist and Bengtsson (1970) described a dust-settling event reaching southern Sweden in the winter of 1969 when dust arrived from south Ukraine. According to Franzén and Hjelmroos (1988), the dust of Danish origin fell with snow in the Gothenburg area in January 1987. Franzén (1989) also described an event in October 1987, when rusty-coloured dust fell off the west coast of Sweden, which was associated with dust storms in Morocco and Algeria.

Franzén et al. (1994) again reported an intense Saharan dust storm event in Scandinavia. In March 1991, the dust of North African origin covered the European continent from Sicily to Finland, covering an area of about 320 000 km². According to Franzén et al. (1995), the earlier bloody rain of 1901 had a similar intensity in Northern Germany, the African origin of which had also been confirmed earlier (Valentin, 1902).

Hongisto and Sofiev (2004) reported a dust storm event of September 2001, which was also observed in Estonia, Finland, and Sweden. The episode lasted for about a week and was caused by a stationary Siberian maximum with a stable anticyclonic flow that carried unusually warm and dusty air from the semi-arid Central Asia, from the Aral-Caspian region. According to their model calculations, the source was the Ryn Peski Desert of Kazakhstan. The meteorological background for such events is a steep pressure gradient between the high-pressure centre over the Eastern European Plain and the low-pressure region situated over the Norwegian coast towards Germany. Also, Hongisto and Sofiev (2004) modelled dust storm events of Caspian and Saharan origin affecting Finland, finding that during the period between 1967 and 1988, dust material from the Caspian region and, in some cases, from the Sahara reached the region relatively frequently. The seasonal distribution of these events is typically limited to autumn and winter for the Caspian sources, while the Saharan events have a winter-spring occurrence. They found that the overall maximum of dusty days occurred during March. In the Aral Sea region, constantly changing anthropogenic influences, changes in agricultural production and land use are

combined with natural dust emissions. Results by Xin and Sokolik (2016) suggest that anthropogenic impacts were dominated by dust storm events controlled by natural processes by the 2010s.

In this paper, we present dust storm events reaching Finland identified based on numerical simulation data available from 1980 to the present, verified by a multistep evaluation process. Our aim was to provide evidence of the long-range transport of Saharan dust to Finland, and to investigate the frequency, temporal distribution, meteorological background, transport directions and potential source areas of dust storm events reaching the Nordic atmosphere.

2. Methods

2.1. Study area

Finland is located in Northern Europe, approximately 4,800 km (3,000 miles) away from the Sahara Desert. Its climate is classified as subarctic, with long, cold winters and short, warm summers. The area is affected by several different air masses, including Arctic air from the north, Atlantic air from the west, and continental air from the east. In the whole country, the wind blows most commonly from the southwest. Occasionally southerly winds can bring warm air to Finland, especially during the transition between winter and spring. These winds can cause significant temperature changes and bring warm and moist air from the Mediterranean region, which can bring precipitation and raise humidity levels. Overall, the frequency of southerly winds in Finland varies depending on the season and weather patterns.

Finland is facing some vulnerabilities to the impacts of climate change. The annual Finnish mean temperature has risen approximately 2 °C since the 1880 s, and this rise in temperature was found statistically significant by Mikkonen et al. (2015). Permafrost exists in Finland in Lapland palsa mires and arctic hills, yet larger permafrost areas in Sweden, Norway, and Siberia are vulnerable to permafrost thaw causing multiple cross-border effects and damage to infrastructure and releasing greenhouse gases into the atmosphere (Meinander et al., 2022a). The variations in the frequency of the dust storm events studied will also allow us to investigate changes in meridional heat transport, which has a significant impact on the region, and provide an opportunity to understand future situations better.

2.2. Satellite and meteorological observation, and numerical simulations

Due to frequent cloud cover and dilution of dust concentrations after long-range transport, aerosol optical depth data for Finland make it difficult to apply satellite measurements to the identification of Saharan dust events. Daily area-averaged means of NASA's MERRA-2 (Modern-Era Retrospective analysis for Research and Applications, Version 2) dust column mass density data (M2T1NXAER.5.12.4) from NASA Goddard Earth Sciences Data Information Services Center (GES DISC) via Giovanni were calculated from the hourly data series for Finland country shape file. Previous studies have confirmed that at higher latitudes, MERRA-2 dust column mass density data allowed the identification of Saharan dust storm events (e.g., Saharan dust events in Iceland: Varga et al., 2021). We handled the episodes when atmospheric dust appears in MERRA-2 simulations over parts of Finland as potential dust storm events. In the article, we defined as dust storm events those episodes for which there was clear evidence that long-range air masses containing mineral dust reached the Finnish region, but this does not imply that the surface atmospheric dust concentration is elevated, only that dust has appeared in the atmosphere. In the vast majority of cases, small amounts of relatively high levels of particulate matter at the surface are not detectable and do not cause significant direct reductions in irradiance (especially since synoptic situations responsible for dust transport are often associated with increases in cloud cover).

Dust column mass density is a measure of the amount of dust per unit of area [kg/m²]. Higher values indicate that there is more particulate

matter per unit area of the air column. Every outlying peak higher than 5×10^{-5} kg/m² of the area (Finland) averaged dust column mass density time series was handled as a date of potential dust episode. (The 5×10^{-5} kg/m² threshold is set on the basis of seasonally varying monthly smoothed values. In the absence of a dust storm event, this value is typically not exceeded.)

All the dates of these peaks were selected for an additional multistep verification process to provide multiple independent confirmations of the atmospheric presence of mineral dust over Finland. This multistep verification process included the usage of: (1) satellite images of Meteosat level 1.5 data (archived in the EUMETSAT Data Centre, derived from MVIRI (Meteosat Visible and Infrared Imager on Meteosat-2 to Meteosat-7) and SEVIRI (Spinning Enhanced Visible and Infrared Imager on Meteosat-8 to Meteosat-10)) and NASA Terra and Aqua MODIS true colour images to visually detect dust plumes on the satellite images, (2) satellite measurements (Aerosol Index values of NASA's TOMS, AURA and OMI measurements (available from 1979), Aerosol Optical Depth data of NASA's Terra and Aqua MODIS measurement (from 2000 and 2006, respectively) to quantifiable verify the elevated dust amount, (3) CALIPSO aerosol v4.10 subtype vertical profiles (<https://www-calipso.larc.nasa.gov/>) to verify the presence of mineral dust in the air column, and (4) MERRA-2 dust column mass density maps. Using maps based on MERRA-2 simulations as a last step, the outliers in the time series were checked to see if they were not just the product of a local dust emission episode, but whether a continuous (typically south-north) dusty air mass actually appeared on the maps. In cases where the dust plume was also visible in satellite images on the days preceding the time series peak, satellite measurements confirmed the presence of atmospheric dust coming from the direction of the potential source areas, the vertical profiles of CALIPSO measurements passing through the area showed the presence of mineral dust and the mapping of MERRA-2 data showed the northward flow of dust-laden air masses from the source areas, then the dust plume events were accepted. Due to data availability, it was not always possible to integrate all independent confirmations.

For the days of the identified episodes, surface particulate matter PM10 (and partly PM2.5) daily maximum of 1-hour averages were also analysed. Data from the Luukki background station (N60.31°, E24.68°, 64 m a.s.l.) were obtained from the Finnish Meteorological Institute open data (Creative Commons Attribution 4.0 International License (CC BY 4.0)) for the background area of Luukki was from the Helsinki Region Environmental Services HSY Air quality measurement network of the Helsinki metropolitan area..

To define the governing synoptic meteorological patterns of dust events, geopotential height, meridional and zonal wind components and wind vector maps were compiled at 700 hPa by using the daily mean composite application of the Earth System Research Laboratory at the United States National Oceanic and Atmospheric Association (NOAA) (<https://www.esrl.noaa.gov/psd/>). The value of 700 hPa was chosen because it has been observed in previous Saharan dust storm events in Europe that dust transport is typically most likely to occur at this level. In the case of Finland, dust was observed at both lower and higher altitudes due to the combined effect of greater distance and more source areas. However, precisely because of the relatively long transport period and the constantly changing dust transport altitudes, and for better comparability, we did not apply multiple (or different) geopotential levels for the synoptic analyses. Surface air temperature anomalies (based on 1981–2010 climatology) were also calculated using the gridded NCEP/NCAR (National Centers for Environmental Protection/National Center for Atmospheric Research) Reanalysis Project dataset (Kalnay et al., 1996).

Multiple endpoints from different heights (from 500 to 6000 m a.s.l.) were used during the 96–168 h backward-trajectory analyses, performed by NOAA HYSPLIT (HYbrid Single-Particle Lagrangian Integrated Trajectory) model to determine the main dust transport pathways (Stein et al., 2015; Rolph et al., 2017). The starting altitude for the backward

trajectories was chosen to best fit the calculated path to the dust plumes of the modeled MERRA-2 maps. This allowed us to assign a typical surface elevation to each episode, i.e. the height at which the dust plume appeared above Finland. Due to the typical southern location of the potential source areas and the dusty air masses that reach the south more frequently, the trajectory calculations were primarily based on back-trajectories from the southern regions of the country. But to verify the dust storm events, a matrix covering the whole country was used. However, when mapping events, only one trajectory was plotted for a dust storm event. The meteorological input for the synoptic analyses and trajectory models was gathered from the Reanalysis Project dataset (Kalnay et al., 1996) of the NCEP/NCAR.

The trajectory method used to study atmospheric dust transport has limitations, considering that it is based only on velocity calculations. It is much simpler than the 4d Eulerian numerical dust transport approach, which is based on complex interactions between dust and the atmosphere, including emission, depositional mixing, and vertical and horizontal transport.”.

2.3. Synoptic meteorological background of dust events

Composite means of 700 hPa geopotential heights, zonal and meridional wind patterns, wind vectors of the different types were also determined by using a daily mean reanalysis database (Reanalysis Project dataset of the NCEP/NCAR), same as used during trajectory calculations to provide a consistent meteorological background. Simultaneously, surface air temperature anomaly maps were also compiled for every type of dust event to quantify the warming effects of these episodes.

3. Results

3.1. Dust events: Temporal patterns and trajectories

A total of 86 long-range dust storm events affecting Finland were identified from 1980 to October 2022 after a multi-stage verification process. The MERRA-2 mass density peak data, the large-scale map data from the simulations, and the satellite imagery all consistently confirmed the presence of dust from long distances, and the trajectories were also traceable to major dust source regions.

Of the available satellite measurements, TOMS and OMI Aerosol Index data were available from the beginning of the study period, but in many cases these can only be used conditionally for atmospheric dust identification. And unfortunately the TOMS AI spatial coverage is only partly available to apply it for Finland. The use of MODIS AOD data is also affected by uncertainties, due to the frequent cloud cover mentioned above and additional air pollution that makes it difficult to identify particulate matter from long distances. Nevertheless, in a number of cases dust storm events have been adequately supported by these measurements.

The CALIPSO vertical aerosol profile data available since 2006 have indeed confirmed the presence of dust to a large extent. See Table 1 for details of the individual episodes, where confirmation is marked with “+” sign.

The trajectory calculations used to identify dust storm events have shown that not only arid regions in North Africa play a role in the development of these episodes, but also other remote arid-semiarid regions. Dust from the Aral-Caspian and Middle Eastern source regions also appears in Finland. These are also marked on the time series in Fig. 1.

The dust transport paths' heterogeneous nature also reflects the meteorological background variability leading to the events (Fig. 2.). Dust from the Aral-Caspian source areas reaches Finland after 2600–3200 km of transport, from the Middle East after 3200–3800 km, and from the Sahara after 3200 to 6000 (or more) km of long drifts.

The frequency of dust storm events varies considerably from year to

Table 1

Detailed data of identified long-range dust events in Finland. (S: Sahara; AC: Aral-Caspian; ME: Middle East; n.d.: no data; “+”: confirmed by the data source; surface temperature difference is compared to the previous 7-days’).

No.	Date	Source	Type	MERRA-2 peak	MERRA-2 map	Satellite image	Aerosol Index	Aerosol Optical Depth	CALIPSO vertical aerosol profile	PM10 [$\mu\text{g}/\text{m}^3$]	PM2.5 [$\mu\text{g}/\text{m}^3$]	Transport height (m above ground level)	Surface temperature anomaly [°C]	Surface temperature difference [°C]
1	1980.06.02	S	1	+	+	+	n.d.					3000	6.8	4.9
2	1981.04.02	S	2	+	+	+						4500	2.4	4.2
3	1982.07.08	AC	3	+	+	+		n.d.				1500	-1.6	1.6
4	1983.04.03	S	1	+	+	+		+				6000	7.0	5.6
5	1983.08.02	S	2	+	+	+		+				4500	2.7	2.5
6	1984.01.28	AC	3	+	+	+		n.d.				500	-1.3	1.7
7	1984.04.05	S	1	+	+	+		+				4500	3.9	2.8
8	1984.05.16	S	1	+	+	+		+				4500	8.2	9.8
9	1984.10.03	S	1	+	+	+		n.d.				3000	6.7	5.7
10	1984.11.13	S	2	+	+	+		n.d.				3000	-0.7	-0.5
11	1985.03.23	S	1	+	+	+		+				6000	2.3	1.7
12	1985.05.01	S	1	+	+	+		n.d.				2500	1.3	4.9
13	1985.09.07	AC	3	+	+	+		n.d.				1500	0.4	-1.3
14	1986.03.11	ME	4	+	+	+		+				4500	-2.3	-4.4
15	1986.04.27	AC	3	+	+	+		+				1000	5.9	4.8
16	1987.03.07	AC	3	+	+	+		+				2000	-7.6	5.5
17	1987.04.03	S	1	+	+	+		+				4500	1.9	0.6
18	1987.10.28	S	2	+	+	+		n.d.				4000	-2.2	-1.3
19	1987.11.30	S	1	+	+	+		n.d.				3000	3.8	5.6
20	1988.02.29	AC	3	+	+	+		+				500	-3.3	2.0
21	1988.03.22	AC	3	+	+	+		n.d.				1500	0.9	3.9
22	1988.05.12	AC	3	+	+	+		n.d.				3500	3.4	5.0
23	1988.10.14	S	1	+	+	+		+				4000	2.9	1.2
24	1989.02.27	S	1	+	+	+		+				1500	7.5	2.3
25	1989.03.09	AC	3	+	+	+		+				1500	0.4	-2.4
26	1989.04.07	S	1	+	+	+		+				3500	0.7	3.6
27	1989.04.13	S	1	+	+	+		+				4500	10.0	6.1
28	1989.04.27	S	1	+	+	+		+				4500	6.6	4.7
29	1989.06.08	S	1	+	+	+		n.d.				4500	2.2	-1.2
30	1990.03.18	S	2	+	+	+		+				4500	8.4	6.9
31	1991.03.11	S	2	+	+	+		+				2000	1.8	-0.1
32	1993.03.30	S	1	+	+	+		+				3500	0.1	0.6
33	1993.05.16	AC	3	+	+	+		n.d.				1000	5.4	1.0
34	1994.04.08	S	1	+	+	+		n.d.				3000	1.3	-1.1
35	1994.04.14	S	1	+	+	+		n.d.				4500	3.7	1.2
36	1994.04.26	AC	3	+	+	+		n.d.				1500	3.6	2.9
37	1995.03.10	AC	3	+	+	+		n.d.				500	1.4	-1.8
38	1995.03.16	AC	3	+	+	+		n.d.				1500	0.4	0.4
39	1996.04.08	S	2	+	+	+		n.d.				4500	4.6	3.3
40	1996.05.04	ME	4	+	+	+		n.d.				2500	6.0	3.8
41	1996.10.18	S	1	+	+	+		n.d.				3000	0.3	0.7
42	1997.07.01	S	1	+	+	+		+				3000	6.6	5.8
43	1998.05.06	S	1	+	+	+		n.d.				3000	-0.6	-5.4
44	1998.06.08	S	2	+	+	+		n.d.				3000	3.8	3.7
45	1999.04.18	S	1	+	+	+		n.d.		44.0	3000	7.4	4.0	
46	1999.10.31	S	2	+	+	+		n.d.		41.9	3000	2.1	1.4	
47	2000.10.03	S	1	+	+	+		n.d.	cloud	25.6	3000	3.7	2.0	
48	2000.10.17	S	1	+	+	+		n.d.	cloud	20.8	4500	1.3	-1.4	
49	2001.04.24	S	1	+	+	+		+		76.9	3000	6.7	5.2	
50	2001.06.09	AC	3	+	+	+		+		13.4	4000	0.7	0.7	
51	2001.10.16	S	2	+	+	+		n.d.		17.5	2000	3.3	-0.2	

(continued on next page)

Table 1 (continued)

No.	Date	Source	Type	MERRA-2 peak	MERRA-2 map	Satellite image	Aerosol Index	Aerosol Optical Depth	CALIPSO vertical aerosol profile	PM10 [$\mu\text{g}/\text{m}^3$]	PM2.5 [$\mu\text{g}/\text{m}^3$]	Transport height (m above ground level)	Surface temperature anomaly [°C]	Surface temperature difference [°C]
52	2002.04.13	S	1	+	+	+				52.0		5000	4.5	1.8
53	2002.05.13	S	2	+	+	+	+	+		37.0		3000	7.7	4.5
54	2002.07.05	S	1	+	+	+	n.d.			27.0		3000	3.2	3.0
55	2003.03.06	S	2	+	+	+				52.0		6000	-1.0	3.1
56	2003.04.12	AC	3	+	+	+	+	+		36.7		3000	-0.5	3.2
57	2004.04.20	S	1	+	+	+	+	+		34.7		4500	5.6	1.1
58	2004.05.06	S	1	+	+	+				28.4		7000	9.1	4.1
59	2007.03.25	S	1	+	+	+	+	+	+			3500	9.0	3.5
60	2007.05.30	ME	4	+	+	+			+			3000	3.7	-0.4
61	2008.04.03	ME	4	+	+	+	n.d.		+	31.9		4500	4.3	1.8
62	2008.04.06	AC	3	+	+	+			+	18.5		3000	2.9	-0.5
63	2008.05.01	ME	4	+	+	+		cloud	+	19.8		7500	7.0	1.9
64	2008.06.01	S	2	+	+	+	n.d.		+	11.9		3000	3.6	1.9
65	2009.01.28	S	1	+	+	+	n.d.	+	+	15.1		1500	3.5	0.3
66	2009.03.10	S	1	+	+	+	+	n.d.		12.8		3000	-0.7	-1.8
67	2010.05.18	AC	3	+	+	+			+	37.3		1000	8.2	-0.2
68	2011.04.12	S	2	+	+	+			+	5.1		3000	-1.7	-1.2
69	2012.04.19	S	1	+	+	+	+		+	9.0		3000	-1.8	-1.2
70	2013.06.02	S	1	+	+	+	n.d.	cloud	+	17.2		5500	6.2	1.7
71	2014.02.02	S	2	+	+	+	n.d.	cloud	+	14.8		3000	1.1	6.9
72	2014.06.06	AC	3	+	+	+			+	22.4		1000	4.6	3.1
73	2015.03.27	S	1	+	+	+	+	cloud	+	23.6		3000	1.3	1.3
74	2016.02.19	S	1	+	+	+	n.d.		n.d.	10.1		4500	5.3	1.4
75	2018.02.11	S	1	+	+	+	+	+	+	14.4		3000	-0.7	1.2
76	2018.04.09	S	2	+	+	+			+	15.9		4500	4.3	1.4
77	2018.04.16	S	2	+	+	+			+	18.1		3500	6.0	3.5
78	2019.04.27	S	1	+	+	+	+	+	+	17.2		3000	5.9	-2.0
79	2021.02.23	S	2	+	+	+	+	+	+	27.4	23.9	3000	-0.6	3.8
80	2021.05.19	AC	3	+	+	+			+	16.1	12.7	1000	3.8	-1.7
81	2021.06.22	AC	3	+	+	+			+	193.3	44.0	2500	10.6	4.0
82	2022.03.18	S	2	+	+	+	+	cloud	n.d.	35.7	29.0	4000	2.5	-1.6
83	2022.03.24	S	2	+	+	+	+		n.d.	13.4	10.8	2000	2.9	-1.8
84	2022.07.02	S	1	+	+	+			n.d.	21.7	13.5	4000	6.5	-2.3
85	2022.07.12	AC	3	+	+	+	+		n.d.	9.7	2.4	2500	2.6	1.9
86	2022.08.21	AC	3	+	+	+	+	cloud	n.d.	54.8	19.1	2500	4.4	-2.0

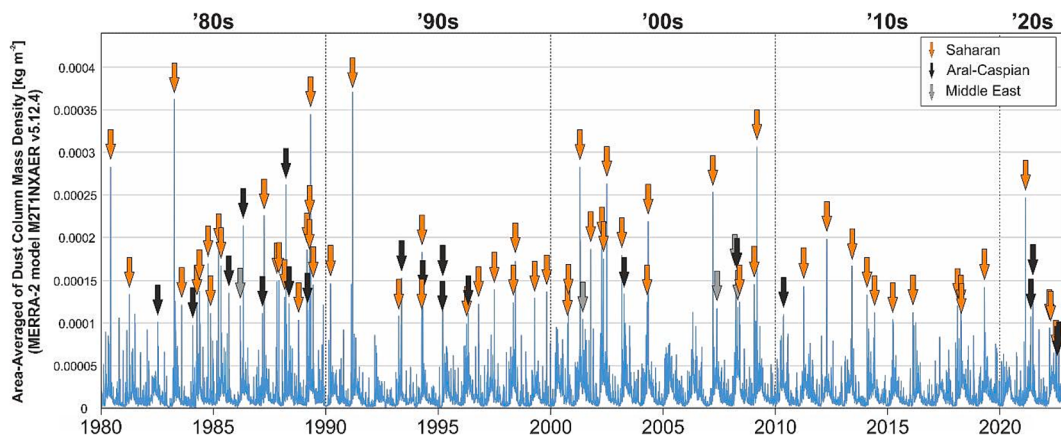


Fig. 1. Area-averaged dust column mass density and the verified dust events in Finland from 1980 to 2022.



Fig. 2. Backward trajectories of long-range dust events identified in Finland between 1980 and 2022 (colour scale indicates the back-trajectory starting point's height above ground level).

year, decade to decade (Fig. 3.). After a peak period in the 1980s ($n = 29$, more than one-third of all events), the number of identified events decreased significantly in the 1990s due to the reduced number of dust storms from Aral-Caspian sources. In the first decade of the 2000s, the three Middle Eastern events and the increase in the number of Saharan dust storms crossing Central and Eastern Europe were observed. In the 2010 s, more Aral-Caspian events were again identified, as well as increased Saharan episodes crossing Western Europe.

Looking at the seasonal distribution (Fig. 4.), there is a clear maximum of dust events in spring (60%), followed by summer (15%) and autumn (13% – 10 of the 11 autumn episodes were from the Sahara). However, the number and proportion of scarce winter events have more than doubled since 2010 compared to the preceding 30 years, but no autumn events were registered during this period. All of the 2010 s winter episodes happened in February and were connected to enhanced atmospheric meridionality-driven dust transport from the Sahara.

3.2. Dust event types

3.2.1. Synoptic types and dust transport routes

Based on key synoptic determinants of backward trajectory and air-mass transport path patterns (e.g., foreside of cyclone, anticyclonic flow of high-pressure centre) and source areas, four different types of episodes were distinguished (Fig. 5.): Sahara-1 (t1 [type-1]: $n = 39$,

Sahara-2 (t2: $n = 20$), Aral-Caspian (t3: $n = 22$) and Middle East (t4: $n = 5$).

Almost half (45%; $n = 86$) of all ($n = 186$) identified dust events were classified as Sahara-1 dust events, in this case, the key driver of northward dust transport is an eastward moving low-pressure system situated over Western or Central Europe. Strong meridional flow at the foreside of the cyclonic centre generates intense dust transport episodes over the central and eastern basins of the Mediterranean Sea and Central Europe, originating from almost all of the northern Saharan dust sources. At the onset of these events, the Mediterranean Sea is experiencing zonal east–west flow conditions at 700 hPa. The meridionality of the transport path is connected to the foreside winds of the low-pressure system and it is enhanced by blocking high pressure systems over the East European Plain. The backward trajectories indicate that the dust reaches Finland at an average altitude of 3750 m above ground level (a.g.l.).

The northern regions of the Sahara, contain several seasonally active dust deposits (Prospero, 2002; Washington et al., 2003; Ginoux et al., 2012), from where dust is transported to the north in the case of this synoptic type. The main sources are the formerly water-covered endorheic basins of the Atlas and the lowlands' seasonally flooded salt lakes in the mountain range's southwestern foothills (Chott Melrhir and Chott Jerid). Additionally, the source areas associated with the debris cones of the north-western slope of the Ahaggar and the extensive wadi system, salt marshes and mudflats of the Tidikelt depression (surrounded by plateaus (Tanezrouft, Plateau du Tademait) and mountains (Ahaggar,

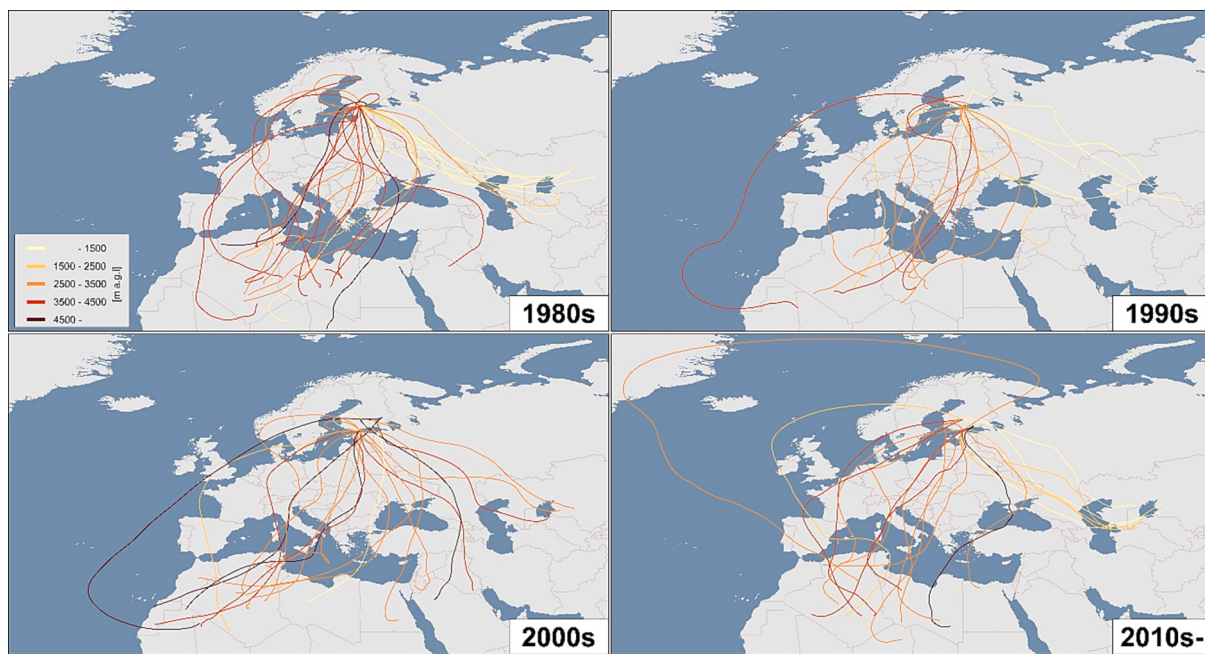


Fig. 3. Backward trajectories by decades of long-range dust events identified in Finland (1980–2022).

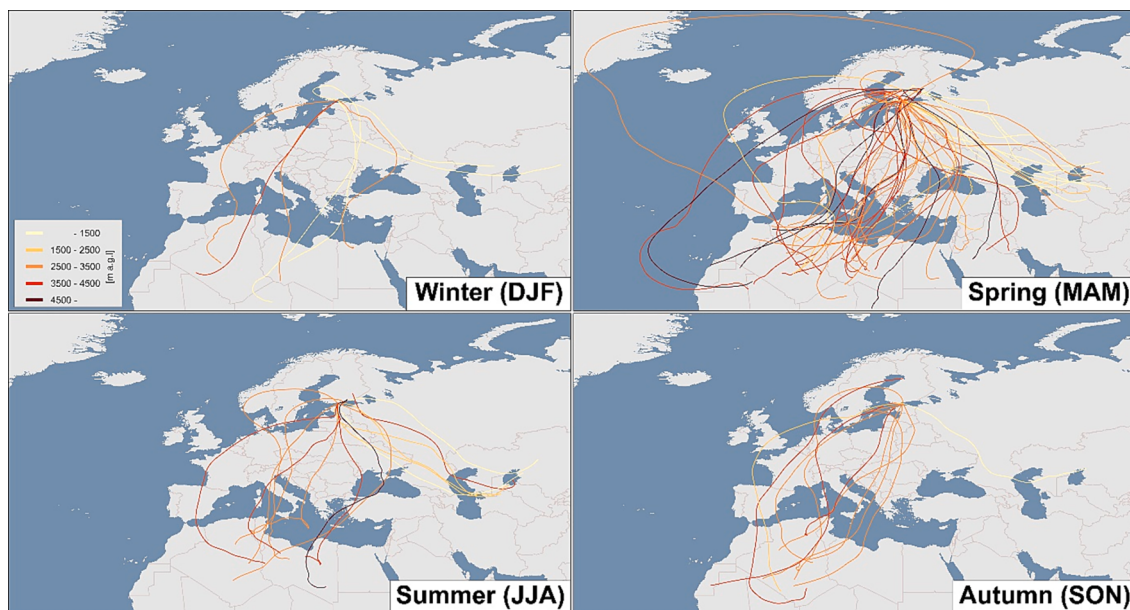


Fig. 4. Backward trajectories by seasons of long-range dust events identified in Finland (1980–2022).

Tassili-n-Ajjer) also play a role in the occasional transport of dust northwards. Dust storms from the slightly more westerly Kireenika and Qattara lowlands are fed by fine-grained debris accumulated in the area's alluvial cones, extensive caldera system and dry lakes.

Enhanced northward dust transport of the 20 (23% of identified dust events) Saharan-2 type dust events is the result of the large pressure gradient between an extensive anticyclone in Central Europe and a westward-moving cyclone over the North Atlantic. Meridional winds carry dust material from (north)western parts of the Sahara northward along the coastline or over Western Europe to the higher latitudes, where the dominant westerlies define the eastward movement of the dust-laden air-masses toward Finland. The dust-laden air masses reach Finland at an average altitude of 3500 m a.g.l.. The north-western Saharan areas defined as typical source areas of Sahara-2 type are

partly the same as those listed for the previous type, with the closed basins of the Atlas and the salt flats of the southwestern foreland of the mountain range being the dominant areas. In addition to these, dust sources in a narrow band on the eastern foothill surfaces of the mountainous areas running along the Atlantic coast in the western Sahara, formed by deposits from periodic water flows and sebkhas (e.g. Sebkha Ijlil) filled by spring flash floods on the foothills of the Adrar Souttouf and Zemmour Massif, are considered to be significant.

In 22 cases (26% of the total), the source area was the wider Aral-Caspian region (from Caspian Lowland dust sources and former Aral Sea deposits – Prospero, 2002; Xi and Sokolik, 2016), from where strong southeasterly winds carried mineral dust into Northern Europe. The flow conditions of these events are determined by a well-defined high-pressure centre over the East European Plain and a northwest-southeast

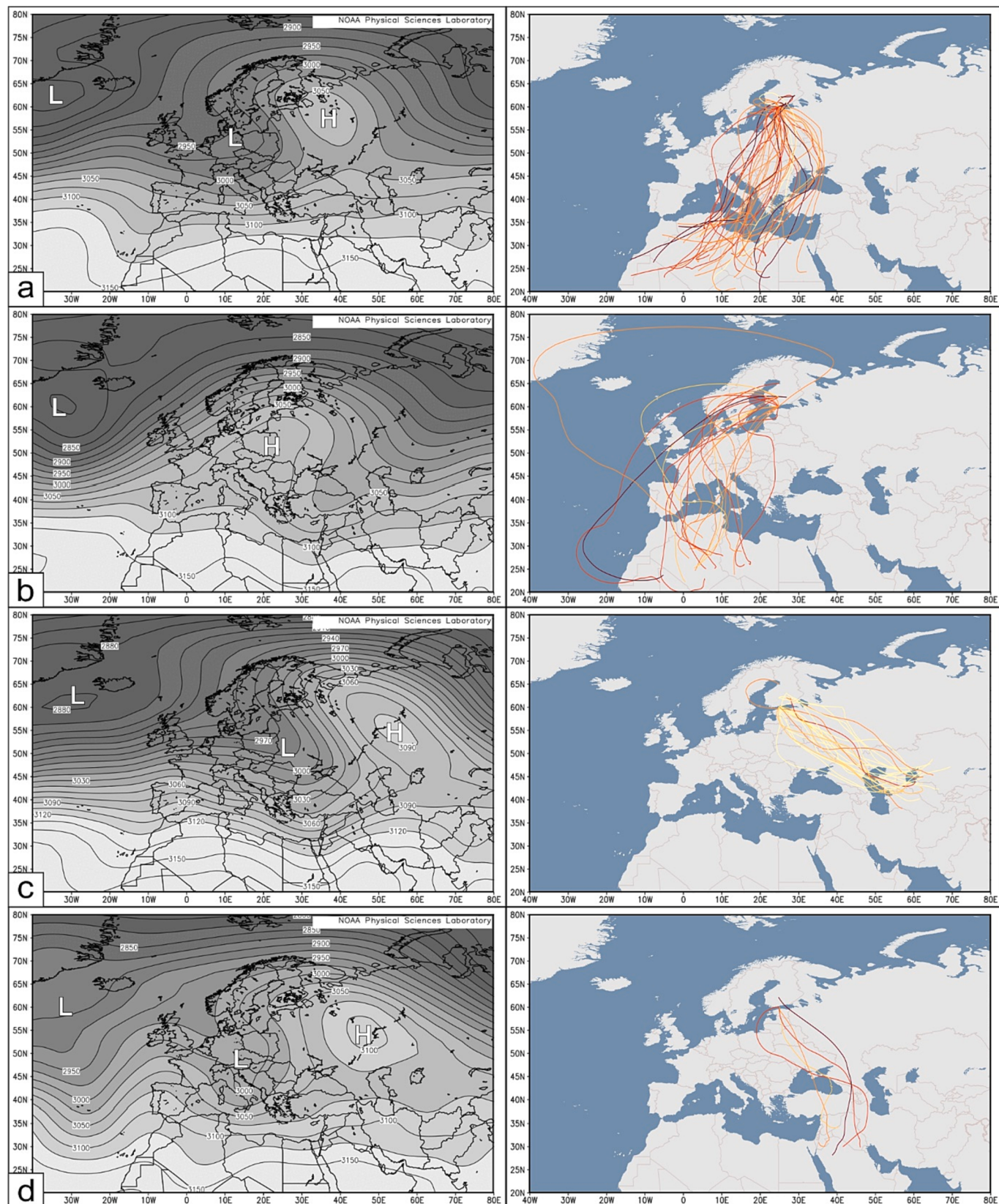


Fig. 5. Synoptic background (mean geopotential height at 700 hPa) and backward trajectories of identified dust events by synoptic types (a: Saharan-1 [t1]; b: Saharan-2 [t2]; c: Aral-Caspian [t3]; d: Middle East [t4]).

atmospheric trough located westwards. The typical altitude of dust transport was the lowest for this type, with dust masses arriving over Finland at an average altitude of 1750 m above the surface. Majority (86%) of the episodes happened during spring ($n = 13$ [59%]) and summer ($n = 6$ [27%]). Numerous source areas are found in the Turanian lowlands and in the northern foothills of the Central Asian mountain ranges. These deflation areas are typically associated with shallow or dry lakes, former lake beds and alluvial cones. Two significant source areas deserve special mention, but unlike previously, they have been created largely as a result of human intervention. On the eastern shores of the Caspian Sea, there is a distinct patchy dust emission region, the Kara-Bogaz Gol, a former, now almost wholly blocked bay of the lake. By the late 1980s, hardly any water-covered area remained in the bay, but this situation has improved, as satellite images show, and there is now more water again. A notorious and typical example of human intervention is the story of the Aral Sea, where the waters of the two major rivers feeding the lake were irrigated and the lake bed turned into a source of dust (Xi and Sokolik, 2016).

Mineral dust material of Middle Eastern source areas could also be identified in five cases. Dust from Syria, Saudi Arabia and Iraq is transported northwards by high-altitude air masses driven by a steep pressure gradient between a Central European low-pressure system and a northwestward moving high-pressure centre (moving northwestward from the Iranian Plateau through the Caspian Lowland to East European Plain). These relatively rare episodes reach northern Europe via high-altitude flows, where they have been identified from backward trajectories at an average altitude of 4400 m above the surface. At the onset of these episodes, intense dust activity was observed in the Middle East. All the Middle Eastern episodes happened in spring. The Middle Eastern source areas tend to be more similar in character to the Sahara than to other Asian source areas (Prospero, 2002; Washington et al., 2003). The Middle Eastern episodes identified in the present study were associated with the Syrian Desert, the Negev, and the floodplain of the characteristically distinct Tigris-Euphrates river system.

3.2.2. Temporal distribution of dust events

The number of identified dust storm events varies considerably from

year to year (Fig. 6.). In the second half of the 1980s, the number of dust storm episodes showed a clear maximum, with 3–6 events detected per year. Thereafter, the typical number of episodes per year is 0–3. In terms of seasonality, the proportion of summer events (17%) should be highlighted in addition to the clear maximum in spring (60%). The number of autumnal dust storms has decreased significantly in the last period, while in contrast, half of the winter events occurred after 2010.

The number of Saharan episodes t1 and t2, also due to the high relative proportion of episodes, matches the seasonal distribution of the total episode population, with a clear maximum in spring for this type, complemented by a peak in October (Figs. 7–8. and Table 2.). In terms of seasonal distribution by decade, the increase mentioned above in February, linked to the last decade, and the disappearance of autumn events are interesting.

3.2.3. Case studies by typical event types

The Saharan dust storm event of October 1987, described by Franzén (1989) was also identified in our analysis and classified as Sahara-1 event, and the Moroccan-Algerian source areas were designated as source areas in both. The intense Saharan dust storm of 1991 described by Franzén et al. (1995) is also included in our list, here classified as Sahara-1 event, with the highest outlier dust column mass density in the time series based on MERRA-2 model results.

Interestingly, the September 2011 dust storm event of Aral-Caspian origin mentioned by Hongisto and Sofiev (2004), and identified here with HYSPLIT, could not be determined based on the MERRA-2 data. This missing episode shows us some of the limitations of the method used here. The multistep verification process confirmed all the presented MERRA-2-based dust events, but there may be events that we have not identified because of model flaws.

In the following, we present examples of intense Saharan dust storm events that represent the types we have defined here for Sahara-1, Sahara-2, Aral-Caspian and Middle East dust transport to Finland (Fig. 9.).

Sahara-1: 2012.04.19.

In mid-April 2012, several dust storms developed on the warm sector of Mediterranean cyclones. One of these was an intense event on 15

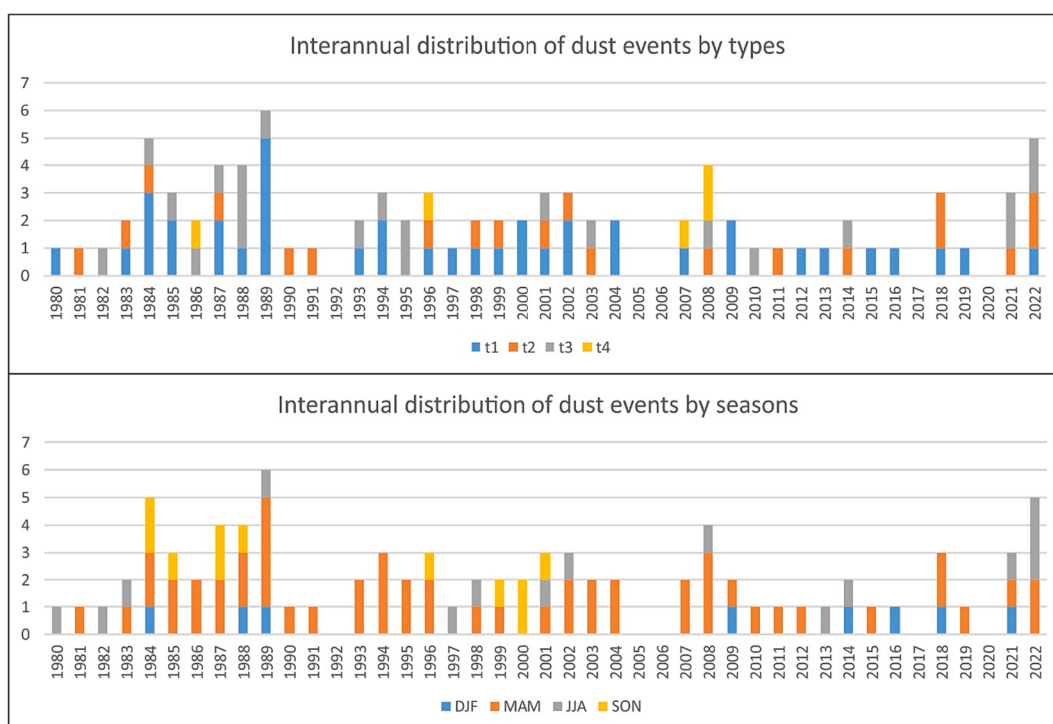


Fig. 6. Annual variations of dust events by types and seasons.

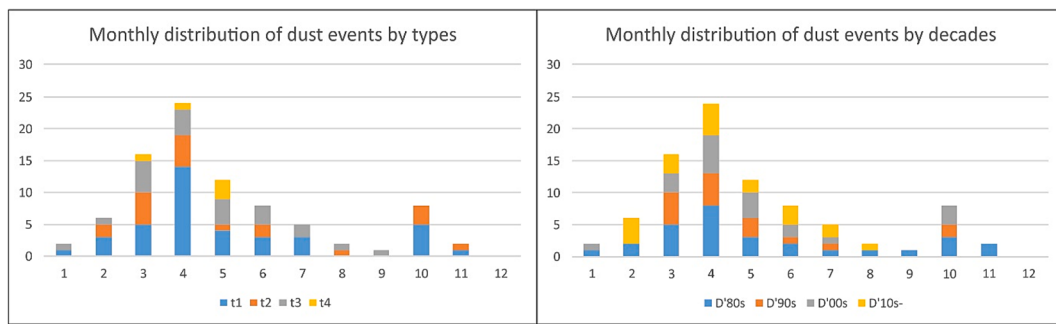


Fig. 7. Seasonal variations of dust events by synoptic types and decades.

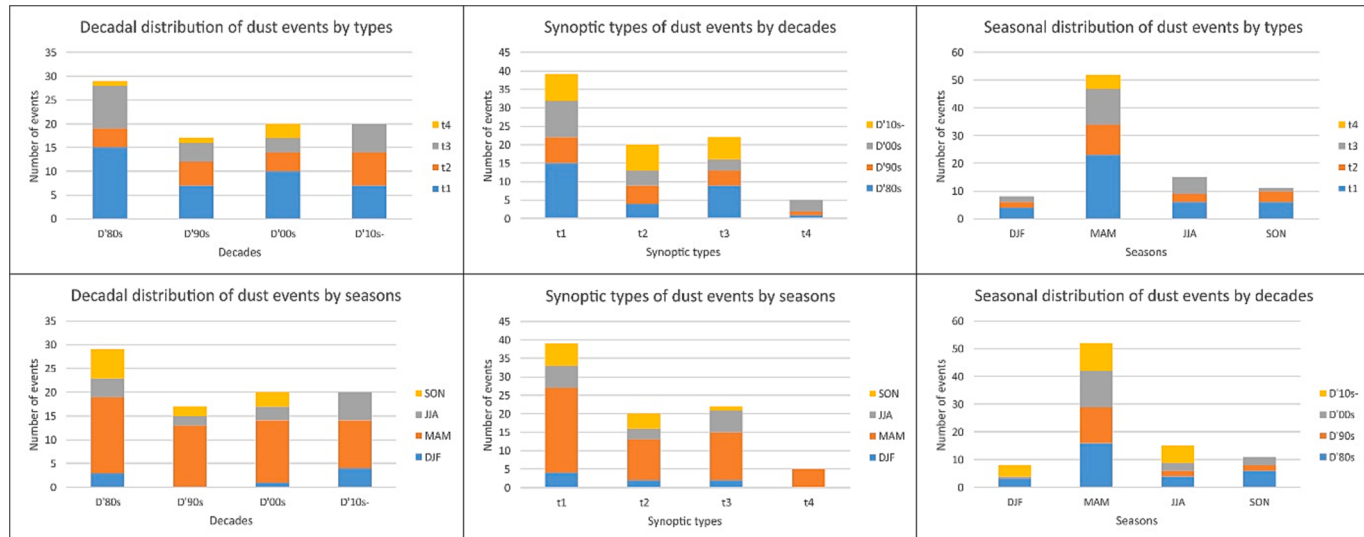


Fig. 8. Distribution of identified dust events by decades, seasons, and synoptic types.

Table 2

Distribution of identified dust events by decades, seasons and synoptic types.

	t1	t2	t3	t4	DJF	MAM	JJA	SON	Total
D'80s	15 (17%)	4 (5%)	9 (10%)	1 (1%)	3 (3%)	16 (19%)	4 (5%)	6 (7%)	29 (34%)
D'90s	7 (8%)	5 (6%)	4 (5%)	1 (1%)	0 (0%)	13 (15%)	2 (2%)	2 (2%)	17 (20%)
D'00s	10 (12%)	4 (5%)	3 (3%)	3 (3%)	1 (1%)	13 (15%)	3 (3%)	3 (3%)	20 (23%)
D'10s-	7 (8%)	7 (8%)	6 (7%)	0 (0%)	4 (5%)	10 (12%)	6 (7%)	0 (0%)	20 (23%)
Total	39 (45%)	20 (23%)	22 (26%)	5 (6%)	8 (9%)	52 (60%)	15 (17%)	11 (13%)	86 (100%)

April, the dust of which drifted northwards on the foreside of a cyclone arriving from the direction of the British Isles. In the days leading up to the dust storm, a multicentre cyclonic field extended from the western Mediterranean basin across central Europe to southern Scandinavia and the foothills of the Urals. The highest daytime temperatures were found in the south-eastern half of Europe, at the front of the cyclonic system, while the north-western half of Europe was much cooler due to several degrees colder air flowing in from the rear of the low-pressure centre. The cold and drier air mass was located to the northwest on the northern side of the cyclonic system, roughly north of the Moscow-Lisbon line. A cyclone swirled over Finland, with cloudy skies but snowfall due to lower temperatures.

Dust from the Northwest Saharan source areas reached Finland as a result of the meridional flow at the front of a large-scale cyclone from the British Isles.

Sahara-2: 2021.02.23.

During the dust storm event of late February 2021, a massive amount of dust reached Europe as a cold front from a high-pressure trough

moving far south from the eastern North Atlantic lifted large amounts of dust over Morocco and Algeria. The warm conveyor belt of the low-pressure system transported the dust northward into Western Europe and towards Scandinavia. The static omega block, evolved from a high-pressure system over Central Europe enhanced the meridional transport of the dust-laden air-masses. (An omega block is formed when a high-pressure area is stuck between two low-pressure areas. Thus, the high pressure, which remains almost stationary, slows down the normal eastward propagation of pressure systems and enhances meridional flow patterns.).

The meteorological situation and the huge amount of dust transported the following year was almost the same. Then, in mid-March 2022, nearly all of Europe was affected by the large-scale Saharan dust storm event.

Aral-Caspian: 2003.04.12.

The strong southeasterly flow, amplified by the high-pressure gradient between the multicentre low-pressure system that dominates Europe's meteorology and the high-pressure centre northeast of the Aral

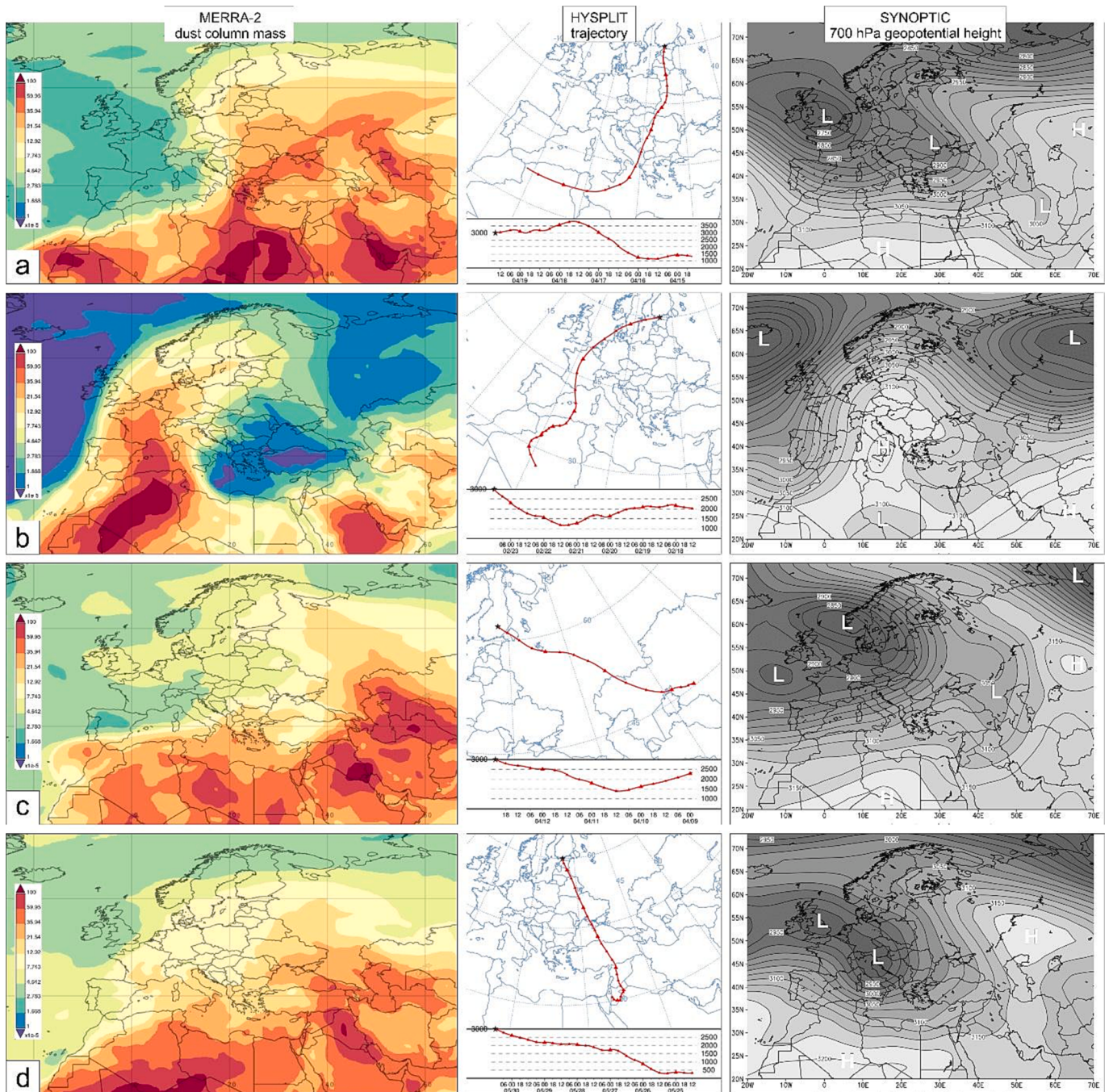


Fig. 9. Daily mean MERRA-2 dust column mass, HYSPLIT backward-trajectories and synoptic background (daily mean 700 hPa geopotential height) for the different Saharan dust event types (a: [t1] 19th April 2012; b: [t2] 23rd February 2021; c: [t3] 12th April 2003; d: [t4] 30th May 2007).

Sea, carried large amounts of dust from the drying lake bed sediments towards Finland in mid-April 2003. Satellite imagery clearly identified local dust storm activity, with the bed of the former Aral Sea and the surrounding now dry, formerly water-covered hot spots actively emitting dust loading the atmosphere with mineral particles even at higher altitudes.

Middle East: 2007.05.30.

Also due to the geographical location of the source area, the selected 2007 Middle East event showed a similar meteorological situation as the Aral-Caspian episode presented above. The late spring and summer is considered the main period of dust storms in the area, when the mineral dust concentration is the highest (Francis et al., 2012). The frontal circulation of the European multicyclonic system determined the southerly

currents prevailing in the area under consideration, which were reinforced by a more extensive inner Asian anticyclone, resulting in an intense, static meridional flow regime between the two centres of action. The slowly eastward-moving low pressure systems in the Mediterranean also produced an intense Saharan dust storm event in the Mediterranean region at the same time as the episode, which later reached the Middle East.

3.2.4. Warm advection during dust events

Meteorological situations that create dust storm events from long distances can significantly change the local weather conditions. The source areas of the studied dust storm events are located far south of Finland, resulting in significant warm advection by winds associated

with enhanced meridional currents. The events with different synoptic situations and air mass movement paths have a specific temperature anomaly pattern (Fig. 10.). The values of the temperature anomaly associated with each episode and the deviations from the previous seven days' averages are given in the Table 1. In areas more affected by dust storm events, these values can be significantly higher than the reported regional averages.

The warm advection values calculated for the coldest winter episodes and higher altitudes exceed those obtained for all events. In all of the identified and presented post-2010 winter dust events in Finland, freezing rain was reported in the affected areas, which may be due to warm advection in the higher layers of the atmosphere. During winter dust storm events, warm advection values calculated at 700 hPa exceeded + 10 degrees Celsius in 2014, 2016 and 2021.

4. Discussion

4.1. Intense dust depositional events and changing climate

Frequency and intensity of dust storms are increasing, see for example, Kok et al. (2023), who have shown that the global dust mass loading has increased $55 \pm 30\%$ since pre-industrial times, driven largely by increases in Asian and North African dust. Possible reasons for increased number of dust intrusions include most of all land use change and desertification of soils in source areas (e.g., Williams and Samara, 2023), coupled with changed climatic condition in these regions, such as increased wind speeds and surface temperature warming (Zhou et al., 2023). In recent years, Europe has been hit several times by widespread Saharan dust storms with intense dust deposition. Such events have been described from the Pyrenees, the Alps, and many other areas of central Europe (Dumont et al., 2023). These were accompanied by events in Finland in February 2021 and March 2022, during which large amounts of dust material were collected thanks to the successful citizen science campaign (Meinander et al., 2022b).

According to Varga (2020), the number of intense winter dust storm events has increased in Central Europe, mainly due to increased jet stream meandering. Linked to this high-altitude mechanism, Francis et al. (2019) and Varga et al. (2021) described changes in the dynamics

of Saharan dust storm events reaching Greenland and Iceland. The waviness of the jet stream can be driven by several processes (Barnes and Screen, 2015), for instance, by the increased warming of the Arctic region, resulting in a decrease in the temperature difference between lower and higher latitudes (Francis and Vavrus, 2012). As a consequence of this decreasing gradient, the jet stream will also become sluggish, slower and more sinuous, with higher amplitude patterns affecting desert regions of lower latitudes, including the Sahara, more frequently. It is worth noting that several alternative theories about the wavy jet stream have been published (Cohen et al., 2014; Screen, 2014; Blackport and Screen, 2020; Kornhuber et al., 2020).

Here, synoptic situations driven by high-altitude currents, cyclonic activity, cut-off low formation and surface flow processes will lead to the formation of intense dust storms, and then the northward-turning stream branching dust-loaded air masses will also reach higher latitudes.

The dust transport of the identified episodes does not necessarily reach the height of the jet stream, but defining the synoptic situations is crucial to understand the various transport patterns and identify their occurrence and changes in time. The dominance of the meridionality of the flow regime and the stationarity of the flow conditions have been caused by the wavy high-altitude jet stream patterns.

4.2. Comparison with Saharan dust events in Southern and Central Europe

Relevant information for the transport of Saharan dust to Finland is provided by the distribution and intensity of dust storm events in the Southern and Central European region, which is a transit area for a significant proportion of the dust storm events presented in this paper, and which has a much larger research literature.

Salvador et al. (2022) observed an increase in Saharan dust transport between 2001 and 2020 in the western Mediterranean. Based on the dataset reported by Varga (2020) for the period 1980–2018, after the frequent dust storms in the 1980s, the number of episodes dropped in the 1990s. Subsequently, more and more Saharan dust has again affected Central Europe, and the last decade has seen a clear increase in the number and intensity of dust storm events. This is particularly true for events that coincide with intense washouts observed in winter. As in

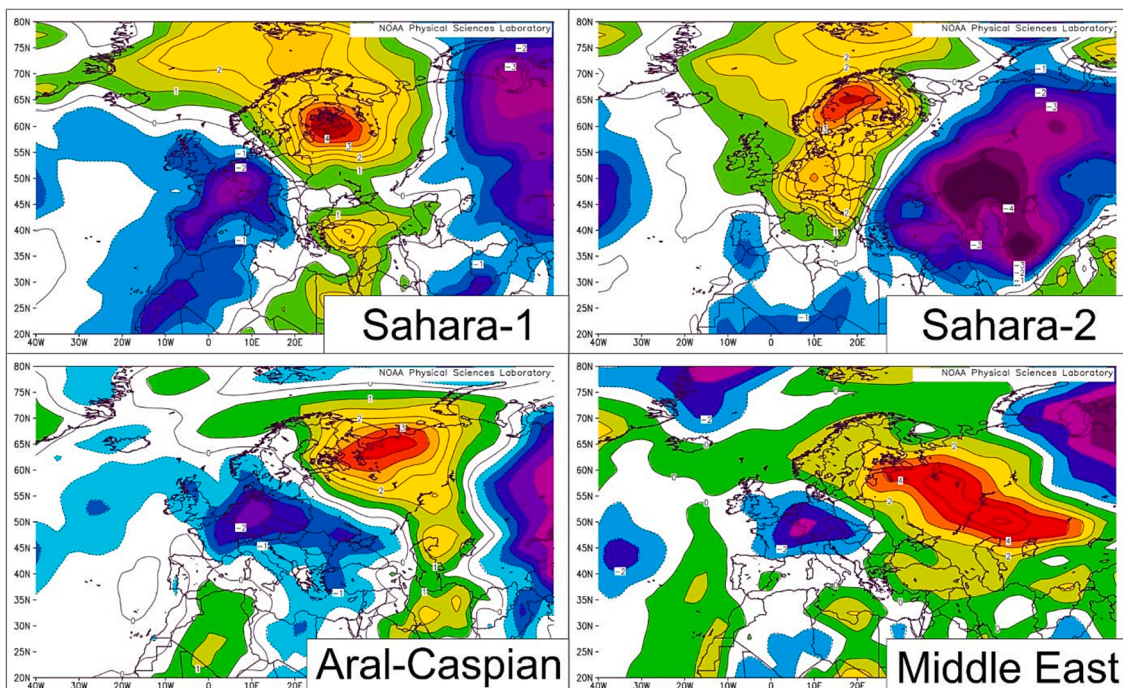


Fig. 10. Surface air temperature anomalies of different types of dust events. (The averages of the different types of events are shown on the maps.).

the case of Finnish dust storm events, the Saharan origin episodes show a decline from an active period in the 1980s to a decline in the 1990s, which more frequent and intense episodes have recently replaced. In terms of their inter-annual distribution, winter episodes have become more frequent in the last decade, in addition to spring and winter maxima.

In terms of seasonality, spring and summer Saharan dust storm events are the most common in Europe. In the Mediterranean, as one moves westwards from the eastern basins, the clear dominance of spring dust storms is replaced by summer events (Varga et al., 2014). A similar shift in trajectories is also observed for Finland, with dust-laden air masses reaching the study area mainly from Central Europe in spring, while episodes from western Europe in the southwest are more frequent in summer and autumn.

There are fewer published data on the transport of particulate matter from the Aral-Caspian region to the north than on the Saharan events. As mentioned in the introduction, Hongisto and Sofiev (2004) attempted to model dust storms of Caspian Sea origin affecting Finland and found that dust material reached the region relatively frequently during the modelled period 1967–1988. The seasonal distribution of these events for Caspian Sea sources is typically limited to autumn and winter. The interannual distribution of the Aral-Caspian events we identified showed a spring and summer maximum.

According to Gikas et al. (2022) arid and semi-arid regions in the Caspian-Aral region (including Atrek River delta, Turan Plain, Takhiyat and Garabogazköl) are the most challenging places for spaceborne passive observations due to the terrain complexity prohibiting the accurate characterisation of the surface reflectance and type. The whole was subject to major landuse changes during Soviet era during the Soviet era. The water of the rivers was irrigated (Amu Darya), and the former Caspian Sea bay (Garabogazköl) was blocked by sand dams. Previous studies based on satellite data and surface observations have clearly shown that these desiccated areas are considered to be the most active sources of dust in the already arid region (Prospero, 2002; Ginoux et al., 2012).

The Aral Sea, located in Central Asia between Kazakhstan and Uzbekistan, was once one of the largest lakes in the world. However, over-irrigation for cotton farming in the region led to a decline in the water levels of the lake, causing it to shrink and eventually split into several smaller bodies of water. The exposed bed of the lake is now a major source of dust, which can be carried by the winds over large distances. The Aral Sea has been reduced in area by about one-tenth in recent decades (becoming a separate desert as Aralkum) and is now considered to be the largest anthropogenic source of dust in the world (Xi and Sokolik, 2016; Banks et al., 2022).

These recent changes in land use and water cover pose serious problems for modelling dust storm events, as many numerical simulations assume the formerly defined dust sources (static topographic depression source map by Ginoux et al. 2001, applied by MERRA-2). Due to the significant underestimation of dust emissions, the shrinking Aral Sea and other desiccated and dry lakes in Central Asia pose serious challenges to the modelling community (Banks et al., 2022).

5. Conclusions

Dust storm events from long distances reaching the Finnish atmosphere were analysed from 1980 to 2022. Using a method based on MERRA-2 Total Dust Column Mass Density data, which underwent multi-stage verification, 86 episodes were identified. In Northern Europe, unlike other regions of Europe, Saharan dust sources are not typically the only major contributors to long-range dust transport events. Among the identified episodes, 59 were associated with Saharan dust sources, 22 with the Aral-Caspian region, and five with Middle Eastern areas. Based on the synoptic positions and dust transport paths, the Saharan dust storm events were further divided into two groups.

It was found that a clear spring maximum characterised the episodes,

but that, similar to other European regions, Finland has experienced an increase in intense winter dust storm events during the last decade. These have been associated with the occurrence of freezing rain observed at the same time as the February episodes, which is driven by warm advection from the high atmosphere.

Over the past decades, there has been a growing identification of Saharan dust storm events across Europe, employing satellite measurements, imagery, numerical simulation data, meteorological analyses, air mass dispersion trajectories, and surface observations. These objective measures exclude subjective forcing factors. It has been observed that both the frequency and intensity of dust storm events have been increasing over the last decade. Considerable variation in inter-annual frequencies was observed among the source areas, which may be due to changes in circulation conditions and the effects of human activity (agriculture and land use changes in Aral Sea region). Based on our results, it is likely that the number of dust storms reaching Finland and the associated frequency of warm convection events will increase in the future.

CRediT authorship contribution statement

György Varga: Conceptualization, Investigation, Writing – original draft, Writing – review & editing. **Outi Meinander:** Conceptualization, Methodology, Writing – review & editing. **Ágnes Rostási:** Conceptualization, Methodology. **Pavla Dagsson-Waldhauserová:** Conceptualization, Supervision. **Adrienn Csávics:** Conceptualization, Methodology, Visualization, Writing – review & editing. **Fruzsina Gresina:** Conceptualization, Methodology, Visualization.

Declaration of Competing Interest

The authors declare that they have no known competing financial interests or personal relationships that could have appeared to influence the work reported in this paper.

Data availability

Data will be made available on request.

Acknowledgement

The research was supported by the NRDI projects FK138692 and RRF-2.3.1-21-2021. The research was funded by the Sustainable Development and Technologies National Programme of the Hungarian Academy of Sciences (FFT NP FTA). The Finnish Meteorological Institute open data (Creative Commons Attribution 4.0 International License (CC BY 4.0)) for the background area of Luukki was from the Helsinki Region Environmental Services HSY Air quality measurement network of the Helsinki metropolitan area.

References

- Banks, J.R., Heinold, B., Schepanski, K., 2022. Impacts of the Desiccation of the Aral Sea on the Central Asian Dust Life-Cycle. *J. Geophys. Res. Atmos.* 127 <https://doi.org/10.1029/2022JD036618>.
- Barnes, E.A., Screen, J.A., 2015. The impact of Arctic warming on the midlatitude jet-stream: Can it? Has it? Will it?: impact of Arctic warming on the midlatitude jet-stream. *Wiley Interdiscip. Rev. Clim. Chang.* 6, 277–286. <https://doi.org/10.1002/wcc.337>.
- Blackport, R., Screen, J.A., 2020. Insignificant effect of Arctic amplification on the amplitude of midlatitude atmospheric waves. *Sci. Adv.* 6 <https://doi.org/10.1126/sciadv.aay2880>.
- Bullard, J.E., Baddock, M., Bradwell, T., Crusius, J., Darlington, E., Gaiero, D., Gassó, S., Gisladottir, G., Hodgkins, R., McCulloch, R., McKenna-Neuman, C., Mockford, T., Stewart, H., Thorsteinsson, T., 2016. High-latitude dust in the Earth system. *Rev. Geophys.* <https://doi.org/10.1002/2016RG000518>.
- Cohen, J., Screen, J.A., Furtado, J.C., Barlow, M., Whittleston, D., Coumou, D., Francis, J., Dethloff, K., Entekhabi, D., Overland, J., Jones, J., 2014. Recent Arctic amplification and extreme mid-latitude weather. *Nat. Geosci.* 7, 627–637. <https://doi.org/10.1038/ngeo2234>.

- Di Biagio, C., Banks, J.R., Gaetani, M., 2022. Dust Atmospheric Transport Over Long Distances. *Treatise Geomorphol.* 259–300 <https://doi.org/10.1016/B978-0-12-818234-5.00033-X>.
- Dumont, M., Gascoin, S., Réveillet, M., Voisin, D., Tuzet, F., Arnaud, L., Bonnefoy, M., Bacardit Peñarroya, M., Carmagnola, C., Deguine, A., Diacre, A., Dürr, L., Evrard, O., Fontaine, F., Frankl, A., Fructus, M., Gandois, L., Gouttevin, I., Gherab, A., Hagenmuller, P., Hansson, S., Herbin, H., Josse, B., Jourdain, B., Lefevre, I., Le Roux, G., Libois, Q., Liger, L., Morin, S., Petitprez, D., Robledano, A., Schneebeli, M., Salze, P., Six, D., Thibert, E., Trachsé, J., Vernay, M., Viallon-Galinier, L., Voiron, C., 2023. Spatial variability of Saharan dust deposition revealed through a citizen science campaign. *Earth Syst. Sci. Data* 15, 3075–3094. <https://doi.org/10.5194/essd-15-3075-2023>.
- Easterling, D.R., Meehl, G.A., Parmesan, C., Changnon, S.A., Karl, T.R., Mearns, L.O., 2000. Climate extremes: Observations, modeling, and impacts. *Science* 289, 2068–2074. <https://doi.org/10.1126/science.289.5487.2068>.
- Francis, D., Eayrs, C., Chaboureau, J., Mote, T., Holland, D.M., 2018. Polar Jet Associated Circulation Triggered a Saharan Cyclone and Derived the Poleward Transport of the African Dust Generated by the Cyclone. *J. Geophys. Res. Atmos.* 123, 11899–11917. <https://doi.org/10.1029/2018JD029095>.
- Francis, D., Eayrs, C., Chaboureau, J.-P., Mote, T., Holland, D.M., 2019. A meandering polar jet caused the development of a Saharan cyclone and the transport of dust toward Greenland. *Adv. Sci. Res.* 16, 49–56. <https://doi.org/10.5194/asr-16-49-2019>.
- Francis, J.A., Vavrus, S.J., 2012. Evidence linking Arctic amplification to extreme weather in mid-latitudes. *Geophys. Res. Lett.* 39, n/a-n/a. <https://doi.org/10.1029/2012GL051000>.
- Franzén, L., 1989. A Dustfall Episode on the Swedish West Coast, October 1987. *Geogr. Ann. Ser. A, Phys. Geogr.* 71, 263–267. <https://doi.org/10.1080/04353676.1989.11880294>.
- Franzén, L., Hjelmroos, M., 1988. A Coloured Snow Episode on the Swedish West Coast, January 1987 A Quantitative and Qualitative Study of Air Borne Particles. *Geogr. Ann. Ser. A, Phys. Geogr.* 70, 235–243. <https://doi.org/10.1080/04353676.1988.11880251>.
- Franzén, L.G., Hjelmroos, M., Källberg, P., Brorström-Lunden, E., Juntto, S., Savolainen, A.L., 1994. The “yellow snowepisode” of northern Fennoscandia, March 1991—A case study of long-distance transport of soil, pollen and stable organic compounds. *Atmos. Environ.* 28, 3587–3604. [https://doi.org/10.1016/1352-2310\(94\)00191-M](https://doi.org/10.1016/1352-2310(94)00191-M).
- Franzén, L.G., Hjelmroos, M., Källberg, P., Rapp, A., Mattsson, J.O., Brorström-Lundén, E., 1995. The Saharan dust episode of south and central Europe, and northern Scandinavia, March 1991. *Weather* 50, 313–318. <https://doi.org/10.1002/j.1477-8696.1995.tb06139.x>.
- Ginoux, P., Chin, M., Tegen, I., Prospero, J.M., Holben, B., Dubovik, O., Lin, S.-J., 2001. Sources and distributions of dust aerosols simulated with the GOCART model. *J. Geophys. Res. Atmos.* 106, 20255–20273. <https://doi.org/10.1029/2000JD000053>.
- Ginoux, P., Prospero, J.M., Torres, O., Chin, M., 2004. Long-term simulation of global dust distribution with the GOCART model: correlation with North Atlantic Oscillation. *Environ. Model. Softw.* 19, 113–128. [https://doi.org/10.1016/S1364-8152\(03\)00114-2](https://doi.org/10.1016/S1364-8152(03)00114-2).
- Ginoux, P., Prospero, J.M., Gill, T.E., Hsu, N.C., Zhao, M., 2012. Global-scale attribution of anthropogenic and natural dust sources and their emission rates based on MODIS Deep Blue aerosol products. *Rev. Geophys.* <https://doi.org/10.1029/2012RG000388>.
- Gkikas, A., Proestakis, E., Amiridis, V., Kazadzis, S., Di Tomaso, E., Marinou, E., Hatzianastassiou, N., Kok, J.F., García-Pando, C.P., 2022. Quantification of the dust optical depth across spatiotemporal scales with the MIDAS global dataset (2003–2017). *Atmos. Chem. Phys.* 22, 3553–3578. <https://doi.org/10.5194/acp-22-3553-2022>.
- Hongisto, M., Sofiev, M., 2004. Long-range transport of dust to the Baltic Sea region. *Int. J. Environ. Pollut.* 22, 72–86. <https://doi.org/10.1504/IJEP.2004.005493>.
- Huneeus, N., Schulz, M., Balkanski, Y., Griesfeller, J., Prospero, J., Kinne, S., Bauer, S., Boucher, O., Chin, M., Dentener, F., Diehl, T., Easter, R., Fillmore, D., Ghan, S., Ginoux, P., Grini, A., Horowitz, L., Koch, D., Krol, M.C., Landing, W., Liu, X., Mahowald, N., Miller, R., Morcrette, J.-J., Myhre, G., Penner, J., Perlitz, J., Stier, P., Takemura, T., Zender, C.S., 2011. Global dust model intercomparison in AeroCom phase I. *Atmos. Chem. Phys.* 11, 7781–7816. <https://doi.org/10.5194/acp-11-7781-2011>.
- IPCC, 2022: Climate Change, 2022. Impacts, Adaptation, and Vulnerability. Contribution of Working Group II to the Sixth Assessment Report of the Intergovernmental Panel on Climate Change [H.-O. Pörtner, D.C. Roberts, M. Tignor, E.S. Poloczanska, K. Mintenbeck, A. Alegría, M. Craig, S. Langsdorf, S. Löschke, V. Möller, A. Okem, B. Rama (eds.)]. Cambridge University Press. Cambridge University Press, Cambridge, UK and New York, NY, USA, 3056 pp., <https://doi.org/10.1017/9781009325844>.
- Kalnay, E., Kanamitsu, M., Kistler, R., Collins, W., Deaven, D., Gandin, L., Iredell, M., Saha, S., White, G., Woollen, J., Zhu, Y., Chelliah, M., Ebisuzaki, W., Higgins, W., Janowiak, J., Mo, K.C., Ropelewski, C., Wang, J., Leetmaa, A., Reynolds, R., Jenne, R., Joseph, D., 1996. The NCEP/NCAR 40-year reanalysis project. *Bull. Am. Meteorol. Soc.* 77, 437–471. [https://doi.org/10.1175/1520-0477\(1996\)077<437:TNYRP>2.0.CO;2](https://doi.org/10.1175/1520-0477(1996)077<437:TNYRP>2.0.CO;2).
- Kok, J.F., Strelcyn, T., Karydis, V.A., Adebiyi, A.A., Mahowald, N.M., Evan, A.T., He, C., Leung, D.M., 2023. Mineral dust aerosol impacts on global climate and climate change. *Nat. Rev. Earth Environ.* 4, 71–86. <https://doi.org/10.1038/s43017-022-00379-5>.
- Kornhuber, K., Coumou, D., Vogel, E., Lesk, C., Donges, J.F., Lehmann, J., Horton, R.M., 2020. Amplified Rossby waves enhance risk of concurrent heatwaves in major breadbasket regions. *Nat. Clim. Chang.* 10, 48–53. <https://doi.org/10.1038/s41558-019-0637-z>.
- Lundqvist, J., Bengtsson, K., 1970. The red snow — a meteorological and pollen-analytical study of longtransported material from snowfalls in Sweden. *Geol. Föreningen i Stock. Förhandlingar* 92, 288–301. <https://doi.org/10.1080/11035897.1970.9626409>.
- Meinander, O., Dagsson-Waldhauserova, P., Amosov, P., Aseyeva, E., Atkins, C., Baklanov, A., Baldo, C., Barr, S.L., Barzycka, B., Benning, L.G., Cvetkovic, B., Enchilik, P., Frolov, D., Gasso, S., Kandler, K., Kasimov, N., Kavan, J., King, J., Koroleva, T., Krupskaya, V., Kulmala, M., Kusiak, M., Lappalainen, H.K., Laska, M., Lasne, J., Lewandowski, M., Luks, B., McQuaid, J.B., Moroni, B., Murray, B., Möhler, O., Nawrot, A., Nickovic, S., O'Neill, N.T., Pejanovic, G., Popovicheva, O., Ranjar, K., Romanias, M., Samonova, O., Sanchez-Marroquin, A., Schepanski, K., Semenkov, I., Sharapova, A., Shevmina, E., Shi, Z., Sofiev, M., Thevenet, F., Thorsteinsson, T., Timofeev, M., Umo, N.S., Uppstu, A., Urupina, D., Varga, G., Werner, T., Arnalds, O., Vuković, Vimić, A., 2022. Newly identified climatically and environmentally significant high-latitude dust sources. *Atmos. Chem. Phys.* 22, 11889–11930. <https://doi.org/10.5194/acp-22-11889-2022>.
- Meinander, O., Alvarez Piedehierro, A., Kouznetsov, R., Rontu, L., Welti, A., Kaakinen, A., Heikkinen, E., Laaksonen, A., 2022b. Saharan dust transported and deposited in Finland on 23 February 2021. In: EGU General Assembly Conference Abstracts, EGU22-4818. <https://doi.org/10.5194/egusphere-egu22-4818>.
- Mikkonen, S., Laine, M., Mäkelä, H.M., Gregow, H., Tuomenvirta, H., Lahtinen, M., Laaksonen, A., 2015. Trends in the average temperature in Finland, 1847–2013. *Stochastic Environ. Res. Risk Assess.* <https://doi.org/10.1007/s00477-014-0992-2>.
- Monteiro, A., Basart, S., Kazadzis, S., Votsis, A., Gkikas, A., Vandebussche, S., Tobias, A., Gama, C., García-Pando, C.P., Terradellas, E., Notas, G., Middleton, N., Kushta, J., Amiridis, V., Lagouvardos, K., Kosmopoulos, P., Kotoni, V., Kanakidou, M., Mihalopoulos, N., Kalivitis, N., Dagsson-Waldhauserová, P., El-Askary, H., Sievers, K., Giannaros, T., Mona, L., Hirtl, M., Skomorowski, P., Virtanen, T.H., Christoudias, T., Di Mauro, B., Trippetta, S., Kutuzov, S., Meinander, O., Nickovic, S., 2022. Multi-sectoral impact assessment of an extreme African dust episode in the Eastern Mediterranean in March 2018. *Sci. Total Environ.* 843, 156861. <https://doi.org/10.1016/j.scitotenv.2022.156861>.
- Prospero, J.M., 2002. Environmental characterisation of global sources of atmospheric soil dust identified with the NIMBUS 7 Total Ozone Mapping Spectrometer (TOMS) absorbing aerosol product. *Rev. Geophys.* 40, 1002. <https://doi.org/10.1029/2000RG000095>.
- Rolph, G., Stein, A., Stunder, B., 2017. Real-time Environmental Applications and Display sYstem: READY. *Environ. Model. Softw.* 95, 210–228. <https://doi.org/10.1016/j.envsoft.2017.06.025>.
- Salvador, P., Pey, J., Pérez, N., Querol, X., Artíñano, B., 2022. Increasing atmospheric dust transport towards the western Mediterranean over 1948–2020. *npj Clim. Atmos. Sci.* 5, 34. <https://doi.org/10.1038/s41612-022-00256-4>.
- Screan, J.A., 2014. Arctic amplification decreases temperature variance in northern mid-to high-latitudes. *Nat. Clim. Chang.* 4, 577–582. <https://doi.org/10.1038/nclimate2268>.
- Shepherd, T.G., 2014. Atmospheric circulation as a source of uncertainty in climate change projections. *Nat. Geosci.* 7, 703–708. <https://doi.org/10.1038/geo2253>.
- Stein, A.F., Draxler, R.R., Rolph, G.D., Stunder, B.J.B., Cohen, M.D., Ngan, F., 2015. NOAA's hysplit atmospheric transport and dispersion modeling system. *Bull. Am. Meteorol. Soc.* <https://doi.org/10.1175/BAMS-D-14-00110.1>.
- Stuut, J.B., Smalley, I., O'Hara-Dhand, K., 2009. Aeolian dust in Europe: African sources and European deposits. *Quat. Int.* 198, 234–245. <https://doi.org/10.1016/j.quaint.2008.10.007>.
- Valentin, J., 1902. Der Staubfall vom 9.–12. März 1901. *Kaiserliche Akademie Wien. Sitzungsber. Mat. Nat. Kl.* 111, 727–729.
- Varga, G., 2020. Changing nature of Saharan dust deposition in the Carpathian Basin (Central Europe): 40 years of identified North African dust events (1979–2018). *Environ. Int.* 139. <https://doi.org/10.1016/j.envint.2020.105712>.
- Varga, G., Újvári, G., Kovács, J., 2014. Spatiotemporal patterns of Saharan dust outbreaks in the Mediterranean Basin. *Aeolian Res.* 15. <https://doi.org/10.1016/j.aeolia.2014.06.005>.
- Varga, G., Dagsson-Waldhauserová, P., Gresina, F., Helgadottir, A., 2021. Saharan dust and giant quartz particle transport towards Iceland. *Sci. Rep.* 11, 11891. <https://doi.org/10.1038/s41598-021-91481-z>.
- Washington, R., Todd, M., Middleton, N.J., Goudie, A.S., 2003. Dust-Storm Source Areas Determined by the Total Ozone Monitoring Spectrometer and Surface Observations. *Ann. Assoc. Am. Geogr.* 93, 297–313. <https://doi.org/10.1111/1467-8306.9302003>.
- Williams, C.G., Samara, F., 2023. Changing particle content of the modern desert dust storm: a climate × health problem. *Environ. Monit. Assess.* 195, 706. <https://doi.org/10.1007/s10661-023-11287-6>.
- Xi, X., Sokolik, I.N., 2016. Quantifying the anthropogenic dust emission from agricultural land use and desiccation of the Aral Sea in Central Asia. *J. Geophys. Res. Atmos.* 121, 12–270. <https://doi.org/10.1002/2016JD025556>.
- Zhou, Y., Wu, T., Zhou, Y., Zhang, J., Zhang, F., Su, X., Jie, W., Zhao, H., Zhang, Y., Wang, J., 2023. Can global warming bring more dust? *Clim. Dyn.* 61, 2693–2715. <https://doi.org/10.1007/s00382-023-06706-w>.